Journal of Power Sources 183 (2008) 518–523

Contents lists available at ScienceDirect

Journal of Power Sources

journal homepage: www.elsevier.com/locate/jpowsour

# Effect of CaO concentration on enhancement of grain-boundary conduction in gadolinia-doped ceria

Pyeong-Seok Cho[a], Sung Bo Lee[b], Yoon Ho Cho[a], Doh-Yeon Kim[b], Hyun-Min Park[c], Jong-Heun Lee[a,*]

[a] Department of Materials Science and Engineering, Korea University, Anam-dong, Sungbuk-ku, Seoul 136-713, South Korea
[b] School of Materials Science and Engineering, Seoul National University, Seoul 151-744, South Korea
[c] New Materials Evaluation Center, Korea Research Institute of Standards and Science, Taeduk Science Town, Daejeon 305-600, South Korea

ARTICLE INFO

*Article history:*
Received 11 February 2008
Received in revised form 9 April 2008
Accepted 9 May 2008
Available online 23 May 2008

*Keywords:*
Gadolinia-doped ceria (GDC)
Grain-boundary conduction
Scavenging effect
Solid oxide fuel cell
Calcium oxide

ABSTRACT

This study examines the effect of calcium oxide (CaO) addition to $Ce_{0.9}Gd_{0.1}O_{1.95}$ (gadolinia-doped ceria, GDC) containing 500 ppm $SiO_2$ on grain-interior and grain-boundary conduction. The GDC can be used as a solid electrolyte for intermediate and low-temperature solid oxide fuel cells. Doping with ≥2 mol% CaO results in a decrease in apparent grain-boundary resistivity at 300 °C from 746.7 kΩ cm to 2.8–3.5 kΩ cm. The total resistivity exhibits a minimum at 2 mol% CaO. Further increase in CaO concentration to 10 mol% results in an increase in grain-interior resistivity from 3.1 to 40 kΩ cm. Although most of the CaO is incorporated into the GDC lattice, a small amount of CaO scavenges the intergranular siliceous phase, which leads to a significant increase in grain-boundary conduction. The increase in grain-interior resistivity at high CaO concentration is attributed to defect association between $V_O^{\bullet\bullet}$ and $Ca_{Ce}''$.



## 1. Introduction

Gadolinia-doped ceria (GDC) is used as solid electrolyte in intermediate- and low-temperature solid oxide fuel cells (IT- and LT-SOFCs) on account of its higher ionic conductivity than yttria-stabilized zirconia (YSZ) [1–11]. In the IT- and LT-regions, the grain-boundary is ~$10^2$–$10^5$ times more resistive than the grain-interior [1,11]. Two main origins for high grain-boundary resistivity are the space-charge layer near the grain-boundary and the siliceous intergranular phase.

A positively charged grain-boundary core is formed in pure GDC materials due to the different formation energies of individual defects [11,12], which lead to the depletion of oxygen vacancies and the accumulation of acceptors near the boundary. On the other hand, it has been reported [1,13–17] that even a few ppm of $SiO_2$ impurity significantly deteriorates ionic conduction across the grain-boundary. It is very difficult to exclude this extrinsic effect completely given that $SiO_2$ is a ubiquitous impurity that can be included during ceramic processing, forming, firing and the operation of fuel cells [1]. In addition, cathode performance can be affected by the siliceous impurity [18].

An improvement in grain-boundary conduction is essential to increase the energy-converting efficiency of LT- and IT-SOFCs. Hence, scavenging of the harmful siliceous phase at the grain-boundary is indispensable. In the well-established stabilized zirconia system, several studies have examined ways to improve grain-boundary conduction [19–26]. Representative approaches include scavenging of the harmful siliceous phase using oxide additives [19–23] and a change in the intergranular phase from a continuous or wetting configuration to a discrete or de-wetting alternative [24–26]. In contrast, studies on improving the grain-boundary conduction in an acceptor-doped ceria system are in their initial stages.

Lane et al. [27] reported that grain-boundary conduction can be enhanced substantially by adding CaO and SrO. The present authors [28,29] briefly examined the corresponding mechanisms. Nevertheless, the incorporation of CaO into the GDC lattice, the effect of CaO addition on the grain-interior and grain-boundary conduction, and the conduction mechanism of CaO-doped GDC specimens are not completely understood. Recently, the present authors [30] reported that the solubility limit of MgO in the GDC lattice is <~0.1 mol% and the siliceous intergranular phase is readily scavenged by a reaction with a second phase, MgO. By contrast, the solubility of CaO in GDC is expected to be relatively high given that the ionic radius of $Ca^{2+}$ (1.12 Å) at a coordination number of 8 is similar to those of $Gd^{3+}$ (1.06 Å) and $Ce^{4+}$ (0.97 Å) [31]. This indicates

* Corresponding author. Tel.: +82 2 3290 3282; fax: +82 2 928 3584.
*E-mail address:* jongheun@korea.ac.kr (J.-H. Lee).

0378-7753/$ – see front matter © 2008 Elsevier B.V. All rights reserved.
doi:10.1016/j.jpowsour.2008.05.041

that the optimum doping concentration for effective scavenging and the scavenging mechanism will both be different on doping with CaO.

In this study, 1–10 mol% CaO is added to a 500-ppm-$SiO_2$-doped $Ce_{0.9}Gd_{0.1}O_{1.95}$ (GDC) specimens, and the effect of CaO doping on grain-interior and grain-boundary conduction is investigated systematically. Major focus is placed on the following: the incorporation of CaO into the GDC lattice, the formation of a second phase, microstructural evolution, the effective concentration window of CaO doping, and the scavenging mechanism.

## 2. Experimental

Pure GDC ($Ce_{0.9}Gd_{0.1}O_{1.95}$, 99.9%, Anan Kasei Co., Japan) was used as a raw material. 500 ppm (by wt.%) $SiO_2$ impurity was added by diluting a $SiO_2$ sol (ST-0, Nissan Chemical Co., Japan) to 0.02 wt.% $SiO_2$ with ethanol, and ball-milling a mixture of GDC powder, dilute $SiO_2$ sol, and ethanol for 24 h. The 0–10 mol% Ca-component was added by dissolving the corresponding amount of $Ca(CH_3COO)_2$ (99%, Sigma–Aldrich Inc., USA) in ethanol and mixing it with 500 ppm-$SiO_2$-doped GDC powder (denoted as GDCSi) by ball-milling. After drying, pulverization and compaction, the specimen was sintered at 1500 °C for 4 h.

Table 1 shows the specifications, compositions, densities and average grain sizes of the samples. After fabricating the Pt electrode, the complex impedance was measured at 300 °C in air using an impedance analyzer (Alpha-N, Nobo control, Germany). Herein, for simplicity, the sintered GDCSi specimens doped with *x* mol% of CaO are denoted as 'GDCSi-*x*Ca'. For example, a GDCSi-5Ca specimen is a 5 mol% CaO-doped $Ce_{0.9}Gd_{0.1}O_{1.95}$ specimen containing 500 ppm $SiO_2$.

To confirm the validity of CaO as a scavenger material, the undoped and 2-mol%-CaO-doped $Ce_{0.8}Gd_{0.2}O_{1.9}$ specimens containing 500 ppm $SiO_2$ was also prepared by ball-milling a mixture of $Gd_2O_3$ (99.99%, Sigma–Aldrich Inc., USA), $Ce_{0.9}Gd_{0.1}O_{1.95}$ powder, and dilute $SiO_2$ sol. The powders were sintered at 1500 °C for 4 h and compacted. The resultant specimens are denoted as 20GDCSi and 20GDCSi-2Ca, respectively.

## 3. Results and discussion

Complex impedance spectra of the undoped and 500 ppm $SiO_2$-doped GDC (GDCpure and GDCSi) specimens were obtained at 300 °C (Fig. 1). The three contributions at low frequency are those from electrode polarization, the grain-boundary and the grain-interior. The grain-interior resistivity ($\rho_{gi}$), apparent grain-boundary resistivity ($\rho_{gb}^{app}$), and total resistivity ($\rho_{tot} = \rho_{gi} + \rho_{gb}^{app}$) are obtained by deconvoluting the impedance spectra. The $\rho_{gb}^{app}$

**Table 1**
Specification, density and average grain size of specimens all sintered at 1500 °C for 4 h

| Specimen | Composition | Density[a] ($g\,cm^{-3}$) | $d_g$[b] (μm) |
|---|---|---|---|
| GDCpure | 10GDC | 7.15 | 2.3 |
| GDCSi | 10GDC + 500 ppm $SiO_2$[c] | 7.21 | 1.8 |
| GDCSi-1Ca | 10GDC + 500 ppm $SiO_2$ + 1 mol% CaO | 7.06 | 4.4 |
| GDCSi-2Ca | 10GDC + 500 ppm $SiO_2$ + 2 mol% CaO | 6.96 | 4.5 |
| GDCSi-5Ca | 10GDC + 500 ppm $SiO_2$ + 5 mol% CaO | 6.74 | 4.8 |
| GDCSi-7Ca | 10GDC + 500 ppm $SiO_2$ + 7 mol% CaO | 6.74 | 7.5 |
| GDCSi-8.5Ca | 10GDC + 500 ppm $SiO_2$ + 8.5 mol% CaO | 6.39 | 6.0 |
| GDCSi-10Ca | 10GDC + 500 ppm $SiO_2$ + 10 mol% CaO | 6.02 | 6.0 |

[a] Apparent density measured by Archimedes' method.
[b] Average grain size measured by linear intercept method.
[c] By weight %.

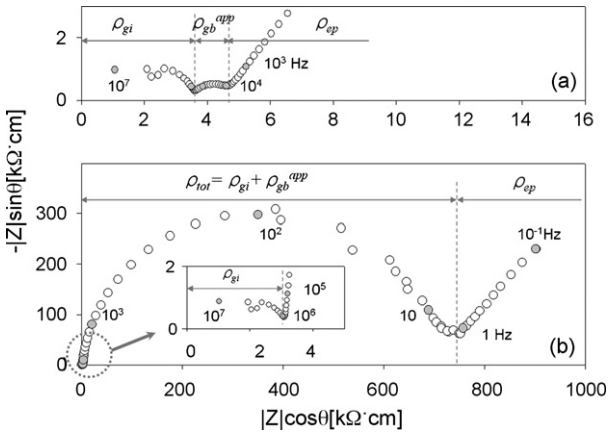


**Fig. 1.** Complex impedance spectra of (a) pure GDC and (b) GDC + 500 ppm $SiO_2$ specimens at 300 °C in air.

value of the GDCpure specimen is 1.2 kΩ cm whereas that of the GDCSi specimen is 747 kΩ cm. The approximately 600 times increase in $\rho_{gb}^{app}$ caused by the addition of 500 ppm $SiO_2$ clearly indicates that the siliceous impurity deteriorates seriously the ionic conduction across the grain-boundary.

CaO (1–10 mol%) was added to the GDCSi specimens, and the complex impedance spectra were measured at 300 °C (Fig. 2). Fig. 3 shows a plot of the $\rho_{gi}$, $\rho_{gb}^{app}$, and $\rho_{tot}$ values deconvoluted from the impedance spectra. The $\rho_{gi}$ value of the GDCSi-1Ca specimen is 3.3 kΩ cm (Fig. 2(a)), which is similar to that (3.2 kΩ cm) of the GDCSi specimen (Fig. 1(b)). On the other hand, the $\rho_{gi}$ value increases gradually to 40 kΩ cm with increasing CaO concentration up to 10 mol%.

A more drastic change is found in $\rho_{gb}^{app}$. The value of the GDCSi-1Ca specimen is 33.1 kΩ cm, which is approximately 4.4% of that obtained for the GDCSi specimen. It decreases further to 2.8 kΩ cm when 2 mol% CaO is added. This corresponds to only 0.38% of the $\rho_{gb}^{app}$ value for the GDCSi specimen. The values remain similar

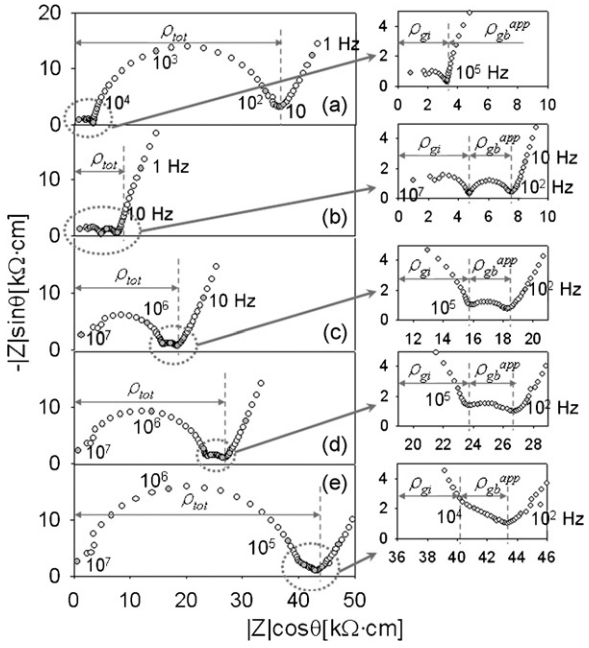


**Fig. 2.** Complex impedance spectra of (a) GDCSi-1Ca, (b) GDCSi-2Ca, (c) GDCSi-5Ca, (d) GDCSi-7Ca and (e) GDCSi-10Ca specimens at 300 °C in air.

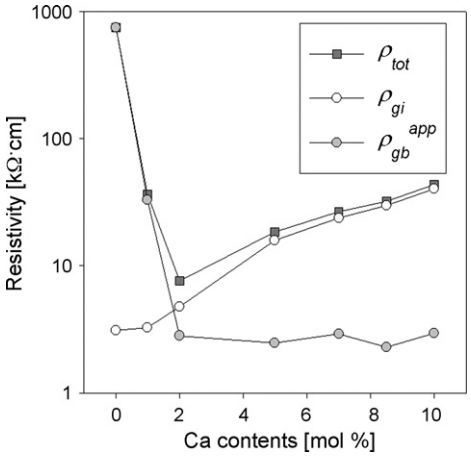


**Fig. 3.** Grain-interior, apparent grain-boundary and total resistivity ($\rho_{gi}$, $\rho_{gb}^{app}$ and $\rho_{tot} = \rho_{gi} + \rho_{gb}^{app}$) of GDCSi specimens at 300 °C as function of CaO concentration.

(3–3.5 kΩ cm) when doped with >2 mol% CaO. This shows that the addition of ≥2 mol% CaO improves the grain-boundary conduction of GDC electrolytes that contain a small amount of siliceous phase but deteriorates the grain-interior conduction. Consequently, the total resistivity ($\rho_{tot}$) exhibits a minimum when doped with 2 mol% CaO (Fig. 3).

The $\rho_{gb}^{app}$ value is calculated from the dimensions of the electrode area ($A$) and sample thickness ($t$), not from the geometry of the grain-boundaries. Therefore, in order to elucidate the real change in the grain-boundary conduction, the specific grain-boundary conductivity ($\rho_{gb}^{sp}$) should be estimated from the geometry of the grain-boundary. Precise estimation of the thickness of the resistive intergranular phase is hampered by the distribution of the space-charge layer, grain-boundary structure, and the configuration of the intergranular phase. Haile et al. [32] suggested that an approximate $\rho_{gb}^{sp}$ value could be calculated from the ratio of the capacitances of the grain-interior and grain-boundary under the following assumptions: (i) a brick layer model; (ii) $\rho_{gb}^{sp} \gg \rho_{gi}$; (iii) grain size ($d_g$) ≫ grain-boundary thickness ($\delta_{gb}$); (iv) permittivity of grain-boundary phase ($\varepsilon_{gb}$) ≅ permittivity of grain-interior phase ($\varepsilon_{gi}$).

The $\rho_{gb}^{sp}$ values are calculated from Figs. 1 and 2, and the results are presented in Fig. 4(a). The $\rho_{gb}^{sp}$ value of the GDCSi specimen is 369.0 MΩ cm and shows that the grain-boundary is $1.2 \times 10^5$ times more resistive than the grain-interior. By contrast, the $\rho_{gb}^{sp}$ value of the 2 mol% CaO-doped GDCSi specimen is 3.2 MΩ cm. The addition of more CaO tends to increase the $\rho_{gb}^{sp}$ value slightly even though there are slight fluctuations in the data (Fig. 4(a)). In order to quantify the effect of CaO addition on the enhancement of grain-boundary conduction, the scavenging factor (SF) is calculated using the following equation:

$$\mathrm{SF} = \frac{\rho_{gb}^{sp}(\mathrm{BS})}{\rho_{gb}^{sp}(\mathrm{AS})}$$

where $\rho_{gb}^{sp}$(BS) and $\rho_{gb}^{sp}$(AS) are the specific grain-boundary resistivity before and after the scavenging reaction. For example, the SF value for the GDCSi-1Ca specimen can be calculated by the ratio between $\rho_{gb}^{sp}$(GDCSi) and $\rho_{gb}^{sp}$(GDCSi-1Ca). The results are shown in Fig. 4(b). It should be noted that the SF values increase abruptly to ~120 when doped with 2 mol% CaO and then decrease gradually to ~60 on the further addition of CaO. This means that the grain-boundary conductivity is increased ~120 times by the addition of 2 mol% CaO. Moreover, the enhancement of grain-boundary conduction is still very high (~60 times) even when 10 mol% CaO is added. This suggests that the significant enhancement in grain-boundary conduction by the addition of ≥2 mol% CaO is not due to a change in grain-boundary density ($D$) but to a change in the physico-chemical properties of the grain-boundary.

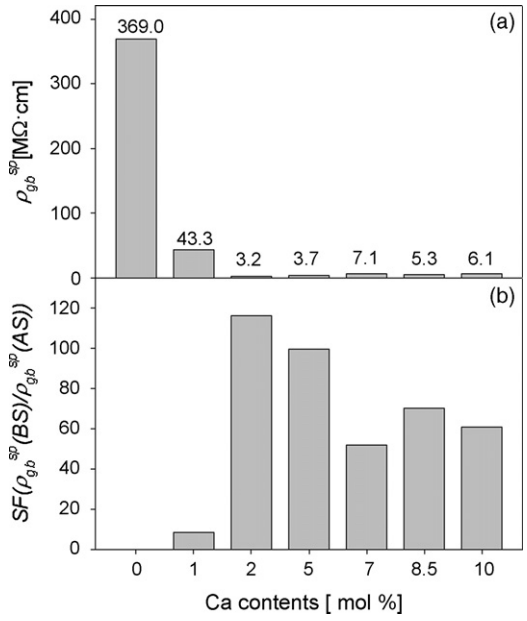


**Fig. 4.** (a) Specific grain-boundary resistivity ($\rho_{gb}^{sp}$) of GDCSi specimens with variation in CaO concentration at 300 °C and (b) ratio between specific grain-boundary resistivity before and after scavenging ($\rho_{gb}^{sp}$(BS)/$\rho_{gb}^{sp}$(AS)).

The X-ray diffraction (XRD) patterns of all the specimens report a pure cubic structure with no secondary phases (data not shown). The lattice parameters of the specimens are calculated using a Si internal standard and are plotted in Fig. 5. In general, the lattice parameters increase with increasing CaO concentration. This indicates that most of the CaO is incorporated into the GDC lattice, which is feasible given that the ionic radius of $Ca^{2+}$ (1.12 Å) at a coordination number 8 is slightly larger than those of $Gd^{3+}$ (1.06 Å) and $Ce^{4+}$ (0.97 Å) [31]. In addition, it was reported [33] that up to ~23 mol% CaO can dissolve into a pure $CeO_2$ lattice. From closer inspection of the data in Fig. 5, however, it is found that the lattice parameters below 2 mol% CaO increase slightly or remain simi-

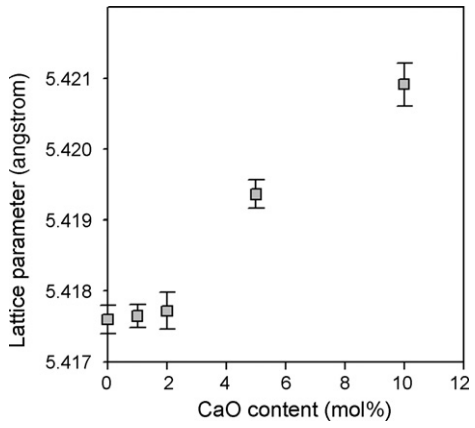


**Fig. 5.** Lattice parameters of GDCSi specimens doped with 0–10 mol% of CaO. Lattice parameters determined using internal Si reference.

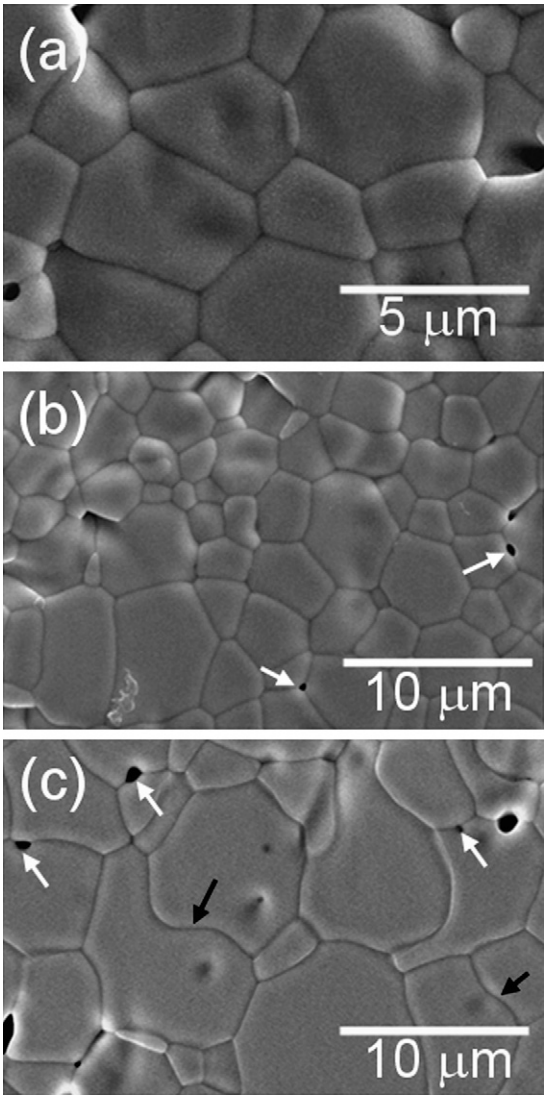


**Fig. 6.** Scanning electron micrographs of (a) GDCSi-2Ca, (b) GDCSi-5Ca and (c) GDCSi-10Ca specimens sintered at 1500 °C for 4 h.

lar. This indicates that the small amount of CaO is mainly used to scavenge a siliceous intergranular phase and that CaO can be incorporated into the interior of GDC after scavenging.

Lane et al. [27] prepared a 1-mol% CaO-doped GDC specimen containing siliceous impurity by sintering at 1450 °C for 4 h. From frequent observations of the second phases containing Si and Ca at the triple-phase boundaries, they proposed scavenging of siliceous impurities by a reaction with CaO. In the study reported here, the presence of a second phase has been checked by scanning electron microscopy (Fig. 6). For the GDCSi-2Ca specimen, it is difficult to find a second phase, and the microstructure is homogeneous. This indicates that the amount of the $SiO_2$-containing second phase is extremely small or absent. A higher sintering temperature (1500 °C) might lead to a higher level of CaO incorporation. Different impurity contents of the specimens or different mixing levels can play another role. In a previous contribution [28], the grain-boundary structures of the GDCSi and GDCSi-2Ca specimens were compared using transmission electron microscopy. The addition of 2 mol% CaO resulted in approximately 50–80% of the grain-boundaries changing from a less coherent random structure to a more coherent faceted one. Therefore, along with nano-scale scavenging of the siliceous phase by CaO, a decrease in siliceous grain-boundary segregation due to the coherent grain-boundary structure was suggested as another possible reason for the enhanced grain-boundary conduction.

Small secondary particles containing $SiO_2$ and CaO were observed at CaO ≥ 5 mol% (indicated by the white arrows in Fig. 6(b) and (c)). This suggests that, although most of the CaO is incorporated into the GDC lattice, there is a very small amount of CaO-containing second phase that readily scavenges the intergranular siliceous phase. The resulting second phase is considered to be thermodynamically stable.

The undulated form of the grain-boundary in the GDCSi-10Ca specimen (see the black arrows in Fig. 6(c)) should be noted. This is representative of a diffusion-induced grain-boundary migration (DIGM) phenomenon. A more detailed study will be needed to confirm this possibility. In the specimen with DIGM, a new solid solution with a different composition is formed behind the migration boundary [34]. Accordingly, the specimen becomes compositionally heterogeneous across the migrating boundary. Nevertheless, the $\rho_{gi}$, $\rho_{gb}^{sp}$, $\Delta E_{gi}$, and $\Delta E_{gb}$ values of the GDCSi-10Ca specimen do not change abruptly. Thus compositional heterogeneity does note have a significant effect on grain-interior or grain-boundary conduction.

Eight complex impedance spectra for 0, 2, 5 and 10 mol% CaO-doped GDCSi specimens were obtained at 300–400 °C, and the apparent activation energy for conduction in the grain-interior ($\Delta E_{gi}$) and grain-boundary ($\Delta E_{gb}$) were calculated from the slopes of the linear plots between $\ln(\sigma T)$ and $(1/T)$. Fig. 7 shows the results for GDCSi and GDCSi-2Ca specimens, whereas the $\Delta E_{gi}$ and $\Delta E_{gb}$ values for all the specimens as a function of CaO concentration are given in Fig. 8. The $\Delta E_{gi}$ value for the GDCSi specimen is $0.723 \pm 0.006$ eV, and increases gradually to $0.998 \pm 0.008$ eV with increasing CaO concentration. In the literature, the grain-interior conductivity in the CaO–$CeO_2$ system shows a maximum at 5–10 mol% CaO and decreases rapidly at 15 mol% [31]. The behaviour was attributed to defect association between $Ca_{Ce}''$ and $V_O^{\bullet\bullet}$. In this CaO–GDC system, $[V_O^{\bullet\bullet}]$ will also increase with increasing CaO concentration. The lattice mismatch between $Ca^{2+}$ (1.12 Å) and $Ce^{4+}$ (0.97 Å) is higher than between $Gd^{3+}$(1.06 Å) and $Ce^{4+}$(0.97 Å), and the electrostatic attraction between $Ca_{Ce}''$ and $V_O^{\bullet\bullet}$ is stronger than between $Gd_{Ce}'$ and $V_O^{\bullet\bullet}$. Therefore, the defect association between $Ca_{Ce}''$ and $V_O^{\bullet\bullet}$ is expected to be easier than between $Gd_{Ce}'$ and $V_O^{\bullet\bullet}$, and $[Ca_{Ce}''–V_O^{\bullet\bullet}]$ will increase with increasing CaO concentration. In this respect, the increase in $\rho_{gi}$ and $\Delta E_{gi}$ values at the higher CaO concentration can be understood by the defect association.

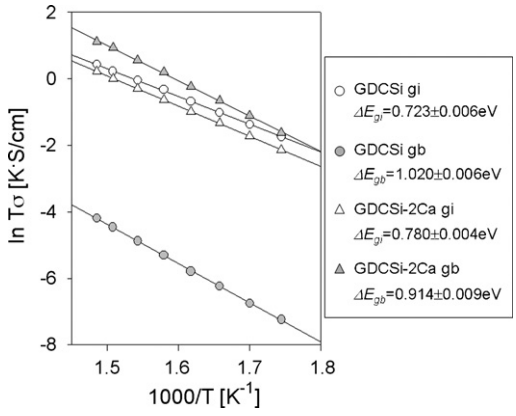


**Fig. 7.** $\ln(\sigma T)$ as function of $1/T$ for (a) GDCSi and (b) GDCSi-2Ca specimens.

The $\Delta E_{gb}$ value of the GDCSi specimen is $1.020 \pm 0.006$ eV, which is substantially higher than the $\Delta E_{gi}$ value ($0.723 \pm 0.006$ eV). Zhang et al. [35] prepared $Ce_{1-x}Gd_xO_{2-\delta}$ ($0.05 \le x \le 0.3$) specimens by oxalate co-precipitation and measured their ionic conductivity. The $\Delta E_{gb}$ and $\Delta E_{gi}$ values for the $Ce_{0.9}Gd_{0.1}O_{1.95}$ specimen were approximately 0.96 and 0.67 eV, respectively; the findings are consistent with those presented here. The slightly higher $\Delta E_{gb}$ value in this study is attributed to greater blocking of ionic conduction by the siliceous intergranular phase.

The $\Delta E_{gb}$ value decreases to $0.914 \pm 0.009$ eV by doping with 2 mol% CaO (Figs. 7 and 8), but increases again to $1.049 \pm 0.014$, $1.085 \pm 0.014$ and $1.141 \pm 0.045$ eV when the CaO concentration is increased to 5, 7 and 10 mol% (Fig. 8), respectively. Two opposite tendencies suggest that CaO plays a dual role in grain-boundary conduction. First, the decrease in the $\Delta E_{gb}$ on doping with 2 mol% CaO can be attributed to removal of the resistive siliceous phase at the grain-boundary by a scavenging reaction. The $\rho_{gb}^{sp}$ values of the 5–10 mol% CaO-doped GDCSi specimens are still much lower than that of the GDCSi specimen, which suggests that scavenging of the siliceous phase is valid. On the other hand, $\rho_{gb}^{sp}$ values at $\geq$5 mol% CaO tend to increase slightly even though the increments are not large (Fig. 4(a)). This cannot be explained by a scavenging reaction because a higher CaO concentration would be more advantageous if it is assumed that the scavenging of a siliceous phase occurs only through a CaO-containing second phase (as indicated in Fig. 6(b) and (c)). The increase in $\rho_{gb}^{sp}$ and $\Delta E_{gb}$ values at >2 mol% CaO can be understood by a change in the space-charge layer. It has been reported that enrichment of oxygen vacancies at the grain-boundary cores in acceptor-doped ceria leads to an accumulation of acceptors with an effective negative charge and a depletion of oxygen vacancies with an effective positive charge near the boundary. The addition of CaO generates $Ca_{Ce}''$ and $V_O^{\bullet\bullet}$ that can alter the structure of the space-charge layer. $Gd^{3+}$ shows an almost perfect match with the $CeO_2$ lattice. By comparison, incorporation of the slightly larger $Ca^{2+}$ into the $CeO_2$ lattice can develop a small amount of lattice mismatch which, in turn, can enhance acceptor accumulation and oxygen vacancy depletion. Moreover, the higher electrostatic interaction between $Ca_{Ce}''$ and $V_O^{\bullet\bullet}$ compared with that between $Gd_{Ce}'$ and $V_O^{\bullet\bullet}$ can also promote acceptor accumulation. In this respect, the change in the space-charge layer can explain the increase in $\rho_{gb}^{sp}$ and $\Delta E_{gb}$ for specimens doped heavily with CaO.

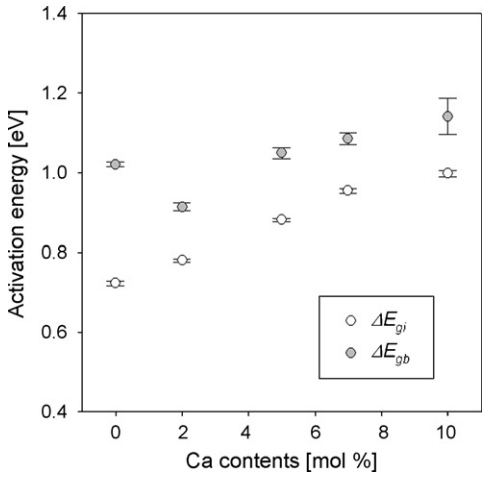


**Fig. 8.** Apparent activation energies for conduction in grain-interior and grain-boundary ($\Delta E_{gi}$ and $\Delta E_{gb}$) determined from plot of $\ln(\sigma T)$ vs. $(1/T)$ at 300–400 °C.

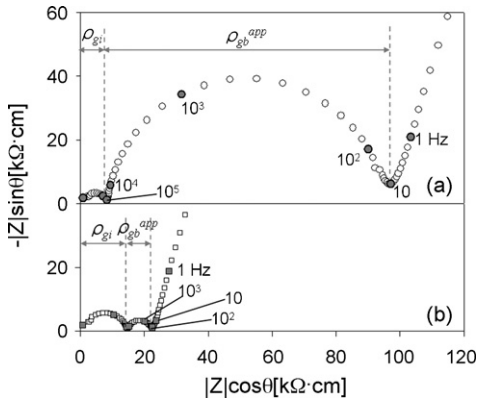


**Fig. 9.** Complex impedance spectra of (a) 20GDCSi and (b) 20GDCSi-2Ca specimens at 300 °C in air.

Since $Ce_{0.8}Gd_{0.2}O_{1.9}$ can be employed as a solid electrolyte for SOFCs, the validity of CaO as a scavenger in $Ce_{0.8}Gd_{0.2}O_{1.9}$ was also investigated. For this, the impedance spectra of undoped and 2-mol%-CaO-doped $Ce_{0.8}Gd_{0.2}O_{1.9}$ specimens containing 500 ppm $SiO_2$ (denoted as 20GDCSi and 20GDCSi-2Ca) at 300 °C were compared (Fig. 9). The $\rho_{gi}$ values of the 20GDCSi and 20GDCSi-2Ca specimens are 8.3 and 14.6 kΩ cm, respectively. These values are higher than that of the GDCSi specimen (3.2 kΩ cm, see Fig. 1(b)). The $\rho_{gb}^{app}$ value of the 20GDCSi specimen is 88.5 kΩ cm (Fig. 9(a)). Although this value is ~12% of that of GDCSi specimen (747 kΩ cm), it is still 10.7 times higher than the $\rho_{gi}$ value (8.3 kΩ cm), which means that the apparent grain-boundary resistivity dominates the total resistivity. The $\rho_{gb}^{app}$ value of the 20GDCSi-2Ca specimen is 7.8 kΩ cm (Fig. 9(b)), which corresponds to 11.3 times increase in the apparent grain-boundary conduction. This shows that the addition of CaO significantly enhances grain-boundary conduction in $Ce_{0.8}Gd_{0.2}O_{1.9}$.

## 4. Conclusions

CaO (1–10 mol%) has been added to $Ce_{0.9}Gd_{0.1}O_{1.95}$ specimens containing 500 ppm $SiO_2$. Doping with $\geq$2 mol% CaO enhances the grain-boundary conduction by up to 120 times. By contrast, the grain-interior resistivity increases with increasing CaO concentration to 10 mol%. The formation of an intergranular second phase containing $SiO_2$ and CaO at 5–10 mol% doping indicates that a small concentration of CaO plays the role of a scavenger, even though most of the CaO is incorporated in the GDC lattice. Scanning election microscopic analysis and the activation energies for conduction in the grain-interior and grain-boundary suggest a dual role for CaO in grain-boundary conduction, namely: (1) mitigation of the siliceous intergranular phase by a scavenging reaction; (2) a change in the space-charge layer into a more resistive configuration. The optimum CaO concentration for an effective scavenging reaction without degrading the grain-interior conduction is 2 mol%.

## Acknowledgement

This work was supported by a Korea Energy Management Corporation Grant (2005-N-PV03-P-02).

## References

[1] B.C.H. Steele, Solid State Ionics 129 (2000) 95–110.
[2] B.C.H. Steele, J. Mater. Sci. 36 (2001) 1053–1068.
[3] V.V. Kharton, F.M. Figueiredo, L. Navapro, E.N. Naumovich, A.V. Kovalevsky, A.A. Yaremchenko, et al., J. Mater. Sci. 36 (2001) 1105–1117.
[4] S.M. Haile, Acta Mater. 51 (2003) 5981–6000.

[5] H. Inaba, H. Tagawa, Solid State Ionics 83 (1996) 1–16.
[6] J.L.M. Rupp, A. Infortuna, L.J. Gauckler, Acta Mater. 54 (2006) 1721–1730.
[7] S.R. Hui, J. Roller, S. Yick, X. Zhang, C. Decès-Petit, Y. Xie, R. Maric, D. Ghosh, J. Power Sources 172 (2007) 493–502.
[8] J.W. Fergus, J. Power Sources 162 (2006) 30–40.
[9] S. Piñol, M. Morales, F. Espiell, J. Power Sources 169 (2007) 2–8.
[10] Z. Shao, S.M. Haile, J. Ahn, P.D. Ronney, Z. Zhan, S.A. Barnett, Nature 435 (2005) 795–798.
[11] X. Guo, R. Waser, Prog. Mater. Sci. 51 (2006) 151–210.
[12] X. Guo, W. Sigle, J. Maier, J. Am. Ceram. Soc. 86 (2003) 77–87.
[13] R. Gerhardt, A.S. Nowick, J. Am. Ceram. Soc. 69 (1986) 641–646.
[14] R. Gerhardt, A.S. Nowick, M.E. Mochel, I. Dumler, J. Am. Ceram. Soc. 69 (1986) 647–651.
[15] T.S. Zhang, J. Ma, Y.J. Leng, S.H. Chan, P. Hing, J.A. Kilner, Solid State Sci. 6 (2004) 565–572.
[16] T.S. Zhang, J. Ma, L.B. Kong, P. Hing, Y.J. Leng, S.H. Chan, J.A. Kilner, J. Power Sources 124 (2006) 26–33.
[17] P. Jasinski, V. Petrovsky, T. Suzuki, H.U. Anderson, J. Electrochem. Soc. 152 (2005) J27–J32.
[18] J.M. Bae, B.C.H. Steel, Solid State Ionics 106 (1998) 247–253.
[19] A.J. Feighery, J.T.S. Irvine, Solid State Ionics 121 (1999) 209–216.
[20] S. Rajendran, J. Drennan, S.P.S. Badwal, J. Mater. Sci. Lett. 6 (1987) 1431–1434.
[21] E.P. Butler, J. Drennan, J. Am. Ceram. Soc. 65 (1982) 474–478.
[22] Y. Shiratori, F. Tietz, H.J. Penkalla, J.Q. He, Y. Shiratori, D. Stöver, J. Power Sources 148 (2005) 32–42.
[23] J.-H. Lee, T. Mori, J.-G. Li, T. Ikegami, M. Komatsu, H. Haneda, J. Am. Ceram. Soc. 83 (2000) 273–275.
[24] J.-H. Lee, T. Mori, J.-G. Li, T. Ikegami, M. Komatsu, H. Haneda, J. Electrochem. Soc. 147 (2000) 2822–2829.
[25] J.-H. Lee, T. Mori, J.-G. Li, T. Ikegami, J. Drennan, D.-Y. Kim, J. Electrochem. Soc. 149 (2002) J35–J40.
[26] Y.-S. Jung, J.-H. Lee, J.-H. Lee, D.-Y. Kim, J. Electrochem. Soc. 150 (2003) J49–J53.
[27] J.A. Lane, J.L. Neff, G.M. Chrisitie, Solid State Ionics 177 (2006) 1911–1915.
[28] P.-S. Cho, S.B. Lee, D.-S. Kim, J.-H. Lee, D.-Y. Kim, H.-M. Park, Electrochem. Solid-State Lett. 9 (2006) A399–A402.
[29] D.K. Kim, P.-S. Cho, J.-H. Lee, D.-Y. Kim, H.-M. Park, G. Auchterlonie, J. Drennan, Electrochem. Solid-State Lett. 10 (2007) B91–B95.
[30] Y.H. Cho, P.-S. Cho, G. Auchterlonie, D.K. Kim, J.-H. Lee, D.-Y. Kim, H.-M. Park, J. Drennan, Acta Mater. 55 (2007) 4807–4815.
[31] H. Yahiro, T. Ohuchi, K. Eguchi, H. Arai, J. Mater. Sci. 23 (1988) 1036–1041.
[32] S.M. Haile, D.L. West, J. Campbell, J. Mater. Res. 13 (1998) 1576–1595.
[33] K. Eguchi, T. Kunisaki, H. Arai, J. Am. Ceram. Soc. 69 (1986) C282–C285.
[34] Y.-W. Rhee, H.Y. Lee, S.-J. Kang, J. Eur. Ceram. Soc. 23 (2003) 1667–1674.
[35] T. Zhang, P. Hing, H. Huang, J. Kilner, Solid State Ionics 148 (2002) 567–573.